

Negative Thermal Expansion and Correlated Magnetic and Electrical Properties of Si-Doped Mn_3GaN Compounds

Ying Sun, Cong Wang,[†] Yongchun Wen, Lihua Chu, and Man Nie

Center for Condensed Matter and Materials Physics, School of Physics, Beihang University, Beijing 100083, China

Fusheng Liu

College of Materials Science and Engineering, Shenzhen University, Shenzhen 518060, China

The negative thermal expansion (NTE) and correlated magnetic and electrical transport properties of $\text{Mn}_3\text{Ga}_x\text{Si}_{1-x}\text{N}$ were investigated. For pure Mn_3GaN , there is a large NTE effect corresponding to the antiferromagnetic to paramagnetic transition. Very interestingly, when partial Ga was replaced by Si, the NTE properties around the magnetic transition were changed. The NTE temperature range was broadened to $\Delta T = 148$ K for $\text{Mn}_3\text{Ga}_{0.75}\text{Si}_{0.25}\text{N}$ and the linear thermal expansion coefficient was estimated as $\beta = -1.4 \times 10^{-5} \text{ K}^{-1}$ (272–420 K). Accordingly, the resistivity also showed a decrease from 327 to 395 K with temperature. With a further increasing Si content to $x = 0.5$, the magnetic transition still occurred, but the NTE effect did not appear. After careful observation, an anomaly was found at around 350 K in a - T , ρ - T , and DSC curves of $\text{Mn}_3\text{Ga}_{0.5}\text{Si}_{0.5}\text{N}$, respectively. This phenomenon strongly implies the close correlation among lattice, spin, and charge in this series materials.

I. Introduction

THE discovery of large negative thermal expansion (NTE) effects in Ge-doped Mn_3CuN compounds has stimulated extensive research on the cubic antiperovskite Mn_3XN ($\text{X} = \text{Cu}, \text{Ga}, \text{Zn}$, etc.).¹ So far, a wide variety of novel physical phenomena have been found in the type of materials, such as superconductivity,^{2,3} giant magnetoresistivity,⁴ nearly zero temperature coefficient of resistivity,⁵ large magnetostriction,⁶ and so on.

As we know, a large and sharp lattice contraction near room temperature exists in pure Mn_3GaN accompanied with an antiferromagnetic (AFM) to paramagnetic (PM) transition.^{7,8} Our previous studies have demonstrated that Ge doping in Mn_3GaN could broaden the sharp lattice contraction.⁸ However, the transition temperature of NTE moves toward the higher temperature region. Generally, the NTE behavior around room temperature is more desirable for actual applications. According to the theory of magnetism, the magnetic transition temperature of Mn_3XN is associated with the number of valence electrons on X and the Mn–Mn distance. Our early studies have demonstrated that more valence electrons on X and larger lattice constant could enhance the magnetic transition temperature⁹ (Y. C. Wen, C. Wang, and Y. Sun, unpublished data). We noticed that Si atom has one more valence electron than Ga,

but smaller. Hence, their combined effect may retain the magnetic transition occurring around room temperature. In addition, Si is assumed to have similar chemical properties with Ge. Thus, the introduction of Si can provide a possibility of broadening the NTE temperature range and also avoid a big change of the transition temperature. Huang *et al.*¹⁰ have reported that the NTE effect moves the toward lower-temperature region and the operative temperature window becomes broader as well, with increasing Si doping content on Ge sites in $\text{Mn}_3\text{Cu}_{0.6}\text{Si}_x\text{Ge}_{0.4-x}\text{N}$.

Antiperovskite Mn_3XN are strongly electron-correlated materials as the metal atoms on X sites provide itinerant electrons on the Fermi level. The feature of the electronic structure for Mn_3XN is that there exists a DOS peak below the Fermi level, E_F . Element Si has one more valence electron than Ga. So, doping with Si atoms strongly increases the number of valence electrons; then, this DOS peak moves to E_F from the low-energy sides while its shape does not change. Hence, the introduction of Si may induce some changes of the structural, electronic, and magnetic transport properties. In this letter, we report the Si-doping effects on the NTE, electrical, magnetic, and thermodynamics properties of Mn_3GaN . It was found that the thermal expansion property of Mn_3GaN was successfully modified by Si doping.

II. Experimental Procedure

Polycrystalline samples $\text{Mn}_3\text{Ga}_{1-x}\text{Si}_x\text{N}$ ($x = 0, 0.25, 0.5$) were prepared by a solid-state reaction using the powders of Mn_2N , GaN, and Si as the starting materials. Stoichiometric amounts of the starting materials were mixed and pressed into pellets. The pellets were wrapped in a Ta foil and then sealed in a vacuumized (10^{-5} Pa) quartz tube. The quartz tube was sintered in a box furnace at 800°C for 96 h, with a couple of intermediate grindings until a pure phase was obtained.

X-ray powder diffraction (XRD) patterns were obtained from a Philips X'Pert PRO X-ray diffractometer (Almelo, the Netherlands). A software named Powder X was used for indexing and lattice constant calculation.¹¹ Structural characterization showed that all of the samples crystallize in the cubic system with $Pm\bar{3}m$ space group. For the measurements of the thermal expansion coefficient (CTE), variable temperature X-ray diffraction was performed on an X'Pert PRO powder diffractometer. The samples were heated to the desired temperature at a rate of 10 K/min and held for 10 min. The XRD patterns at different temperatures were recorded, and then the lattice constants were calculated by indexing all of XRD peaks. The error bar for lattice measurement was evaluated to be 0.0002 Å. The lattice constant variation with temperature is far bigger than the error measured. Thus, the CTE was obtained by $\beta = \Delta a/a\Delta T$ from the slope of a - T curve, as shown in Fig. 1. Previous reports used only a strain gauge to measure the linear CTE of the kind of

L. Schneemeyer—contributing editor

Manuscript No. 26461. Received July 15, 2009; approved October 8, 2009.
 This work was financially supported by National Natural Science Foundation of China (NSFC) (No. 50772008).

[†]Author to whom correspondence should be addressed. e-mail: congwang@buaa.edu.cn

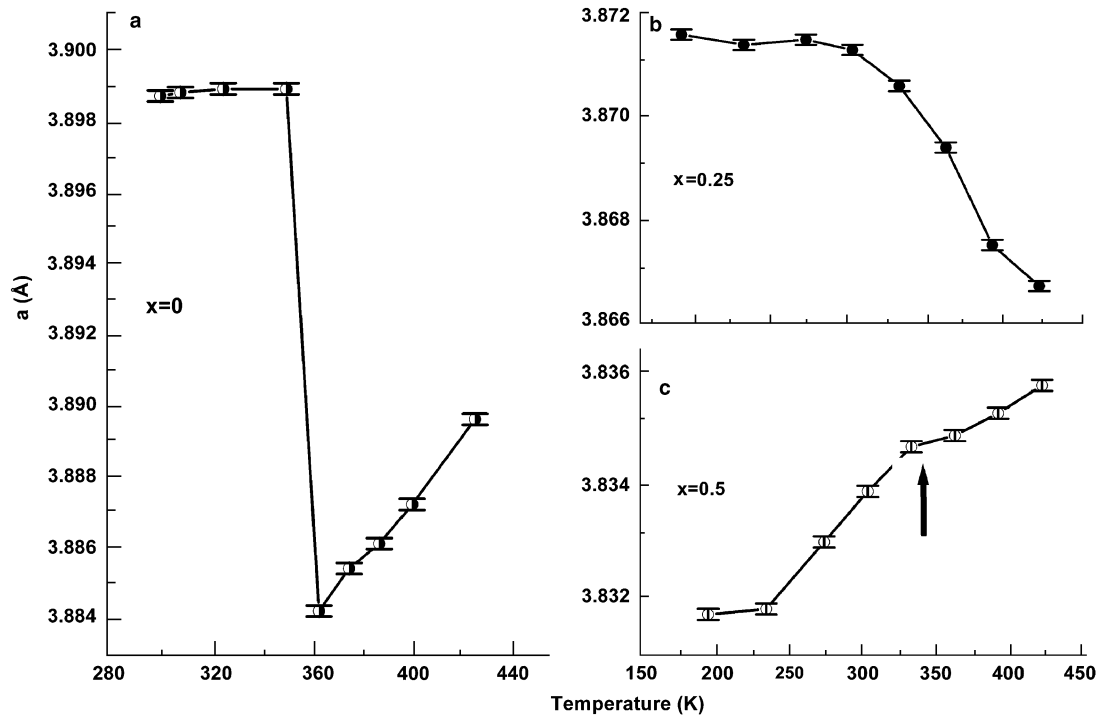


Fig. 1. Temperature dependence of the lattice constants for $\text{Mn}_3\text{Ga}_{1-x}\text{Si}_x\text{N}$ by variable temperature X-ray powder diffraction. (a) for $x=0$; (b) for $x=0.25$; and (c) for $x=0.5$.

materials, which is apparent and inaccurate.^{10,12} Lattice variation is a kind of intrinsic change and excludes the influences of cracks or others. $M(T)$ curves were measured at 50 Oe with a Quantum Design Magnetic Property Measurement System XL5 SQUID susceptometer (Quantum Design Corporate, San Diego, CA), which uses SQUID (superconducting quantum interference device) technology, to achieve superior measurement sensitivity and a dynamic range. Four-probe method was used for the measurement of temperature variation of the resistivity. The sintered polycrystalline samples were cut into a bar shape (1 mm \times 2 mm \times 8 mm) for electrical resistivity measurements and air-dried silver epoxy was used for making the electrical contacts. Thermal analysis was conducted using TAQ200 DSC (TA Instruments Ltd., New Castle, DE) in the temperature range from 180 to 500 K.

III. Results and Discussion

First, the thermal expansion behaviors were measured by variable temperature X-ray diffraction. All of XRD peaks were checked carefully, and with increasing temperature, only the shift of the peaks was found and no new peaks appeared. The lattice constants were calculated at different temperatures by Powder X software. As shown in Fig. 1(a), there exists an abrupt drop of lattice constant (a) for Mn_3GaN starting from 348 K and finishing at 361 K, without breaking the cubic symmetry. Then, we introduced some Si to replace Ga and obtained $\text{Mn}_3\text{Ga}_{0.75}\text{Si}_{0.25}\text{N}$ phase. For $\text{Mn}_3\text{Ga}_{0.75}\text{Si}_{0.25}\text{N}$, the crystalline structure remains in cubic symmetry and the lattice constant at room temperature is 3.8712(2) Å, smaller than Mn_3GaN (3.8988 Å). As Si atom is smaller than Ga, this result indirectly revealed that Si atoms were successfully introduced into Ga positions. Very interestingly, a different thermal expansion behavior was observed for $\text{Mn}_3\text{Ga}_{0.75}\text{Si}_{0.25}\text{N}$, as shown in Fig. 1(b). The lattice constant of $\text{Mn}_3\text{Ga}_{0.75}\text{Si}_{0.25}\text{N}$ first maintains the minor change from 190 to 272 K with increasing temperature. Then, the cubic lattice constant gradually decreases with temperature from 272 to 420 K, i.e. the sharp lattice contraction process in Mn_3GaN was obviously modified by Si doping. The NTE temperature range was broadened to $\Delta T = 148$ K from a quite nar-

row range. The thermal expansion coefficient in the NTE temperature region was determined as about $\beta = -1.4 \times 10^{-5} \text{ K}^{-1}$ (272–420 K). We further increased Si content to $x = 0.5$. Unexpectedly, the NTE behavior disappeared and completely turned positive over the entire temperature range. We repeated the measurement of variable temperature X-ray diffraction and the same result was always obtained. However, there is a deviation for $\text{Mn}_3\text{Ga}_{0.5}\text{Si}_{0.5}\text{N}$ around 350 K, as clearly seen in Fig. 1(c). The linear thermal expansion coefficients are $7.60 \times 10^{-6} \text{ K}^{-1}$ below 350 K and $3.91 \times 10^{-6} \text{ K}^{-1}$ above 350 K, respectively.

To testify the result, we carried out a calorimetric measurement. Figure 2 gives the DSC curves of the samples. For Mn_3GaN , upon heating, a sharp and narrow peak was detected, which is indicative of the first-order phase transition. This is consistent with the thermodynamic view, which refers that the first-order transition is often accompanied by a thermal release and discontinuity of volume change. From the results of the lattice constant, the discontinuous lattice contraction of

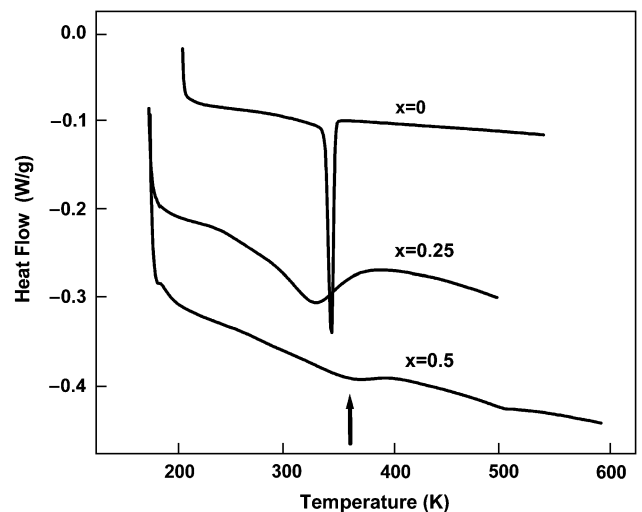


Fig. 2. DSC curves for $\text{Mn}_3\text{Ga}_{1-x}\text{Si}_x\text{N}$.

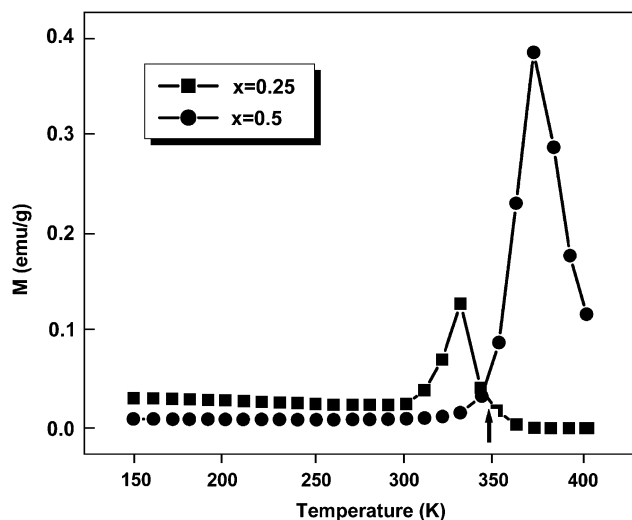


Fig. 3. Temperature dependence of the magnetization for $\text{Mn}_3\text{Ga}_{0.75}\text{Si}_{0.25}\text{N}$ (■) and $\text{Mn}_3\text{Ga}_{0.5}\text{Si}_{0.5}\text{N}$ (●).

Mn_3GaN was modified to continuous after Si was introduced. Therefore, the essence of the phase transition may be changed accordingly by Si doping. As expected, the sharp peak becomes weaker and broader when $x = 0.25$. Moreover, no obvious endothermic peak occurred in the DSC curve of $\text{Mn}_3\text{Ga}_{0.5}\text{Si}_{0.5}\text{N}$. This characteristic reveals that the phase transition may have changed toward the second-order phase transition from the first-order phase transition.

As the NTE property is related to the magnetic transition in this material, the variation of magnetization with temperature was measured. The magnetization curves of $\text{Mn}_3\text{Ga}_{0.75}\text{Si}_{0.25}\text{N}$ and $\text{Mn}_3\text{Ga}_{0.5}\text{Si}_{0.5}\text{N}$ are displayed in Fig. 3, while the magnetic transition of Mn_3GaN has been reported in our early paper.⁸ Similar to Mn_3GaN , the AFM–PM transition occurs with increasing temperature and the transition points T_N , which was defined by the peak position, are 330 and 370 K for $\text{Mn}_3\text{Ga}_{0.75}\text{Si}_{0.25}\text{N}$ and $\text{Mn}_3\text{Ga}_{0.5}\text{Si}_{0.5}\text{N}$, respectively. In order to further understand the Si-doped effects, we investigated the electronic transport properties of $\text{Mn}_3\text{Ga}_{1-x}\text{Si}_x\text{N}$. Figure 4 presents the temperature dependence of resistivity. The resistivity of $\text{Mn}_3\text{Ga}_{0.75}\text{Si}_{0.25}\text{N}$ first exhibits a metallic behavior at low temperature. From 327 K, it continuously decreases with temperature. Until 395 K, the resistivity reaches a minimum and then increases with further increasing temperature. Instead, the resistivity of $\text{Mn}_3\text{Ga}_{0.5}\text{Si}_{0.5}\text{N}$ shows a metallic-like behavior in the entire temperature range. After careful observation, it was found that the increasing rate became slower after 345 K, i.e. there

existed an anomaly in resistivity for $\text{Mn}_3\text{Ga}_{0.5}\text{Si}_{0.5}\text{N}$ at about 345 K, which was in good agreement with their magnetic transition temperature. The $d\rho/dT$ rates are $1.38 \times 10^{-3} \text{ m}\Omega \cdot \text{cm/K}$ below 345 K and $9.95 \times 10^{-4} \text{ m}\Omega \cdot \text{cm/K}$ above 345 K, respectively.

As reported early, the magnetic transition of Mn_3XN is always accompanied by other anomalous features, such as abrupt change of the resistivity and lattice constant.^{13,14} For $\text{Mn}_3\text{Ga}_{0.5}\text{Si}_{0.5}\text{N}$, it is readily noticed that the lattice contraction and abnormal decrease of resistivity did not occur while an obvious magnetic transition occurred. This phenomenon reveals that magnetic transition is not enough for abnormal change in lattice and resistivity. The other reasons need further exploration in the future.

Antiperovskite manganese nitrides are strongly electron-correlated materials. In Mn_3XN , narrow bands are formed near the Fermi level by the strong hybridization between N 2p and Mn 3d orbitals. The occupation of these narrow bands is sensitively changed according to the number of the valence electrons on X site because the X atoms provide the itinerant electrons at the Fermi level.¹⁵ Element Si has one more valence electron than Ga. Thus, the introduction of Si can be considered as one-electron doped in Mn_3GaN followed by geometrical frustration like Ge-doping in Mn_3CuN .¹⁶ Furthermore, Si doping will lead to certain kinds of structural defects due to lattice mismatch, which could sufficiently modify the electronic structure of the material and possibly result in the change of the crystal and spin structures of Mn_3GaN . Ikubo *et al.*¹⁷ have reported that not only a cubic crystal structure but also a AFM^{3g} AFM spin structure are key ingredients of the large magnetovolume effect in the itinerant electron system. In our case, the crystal structure did not change after Si doping. However, the exchange interactions between the nearest neighbor Mn moments may be disturbed in the presence of Si. Thus, spin canting may appear, which gives rise to a relaxor-like behavior.¹⁰ Accordingly, the NTE operation temperature window could be broadened and even completely turned positive with increasing Si content.

IV. Conclusion

The Si-doping effects on the thermal expansion properties of Mn_3GaN were investigated by variable temperature X-ray diffraction. After partial Si doping, the sharp lattice contraction in Mn_3GaN was broadened. For $\text{Mn}_3\text{Ga}_{0.75}\text{Si}_{0.25}\text{N}$, the NTE temperature range reached $\Delta T = 148 \text{ K}$ and the CTE from 272 to 420 K was determined as about $\beta = -2.8 \times 10^{-5} \text{ K}^{-1}$. The NTE effect acted in accord with the AFM–PM transition. Further increasing Si concentration to $x = 0.5$, the AFM–PM transition still occurred. However, the thermal expansion behavior and temperature-dependent resistivity completely turned to be positive. Thus, we think that the magnetic transition is not sufficient to introduce the abnormal change of both the lattice constant and resistivity in the materials. Thermal analysis indicated that for the phase transition, there was a qualitative change from the first order to the second order when doping Si into Mn_3GaN . Further study is deserved for realizing the effects of Si doping and also for developing negative or zero thermal expansion materials, whose specific characteristics are attractive for applications.

References

- ¹K. Takenaka and H. Takagi, "Giant Negative Thermal Expansion in Ge-doped Anti-perovskite Manganese Nitrides," *Appl. Phys. Lett.*, **87**, 261902, 3pp (2005).
- ²T. He, Q. Huang, A. P. Ramirez, Y. Wang, K. A. Regan, N. Rogado, M. A. Hayward, M. K. Haas, J. S. Slusky, K. Inumara, H. W. Zandbergen, N. P. Ong, and R. J. Cava, "Superconductivity in the Non-oxide Perovskite MgCNi_3 ," *Nature*, **411**, 54–6 (2001).
- ³H. Rosner, R. Weht, M. D. Johannes, W. E. Pickett, and E. Tosatti, "Superconductivity Near Ferromagnetism in MgCNi_3 ," *Phys. Rev. Lett.*, **88**, 027001, 4pp (2002).

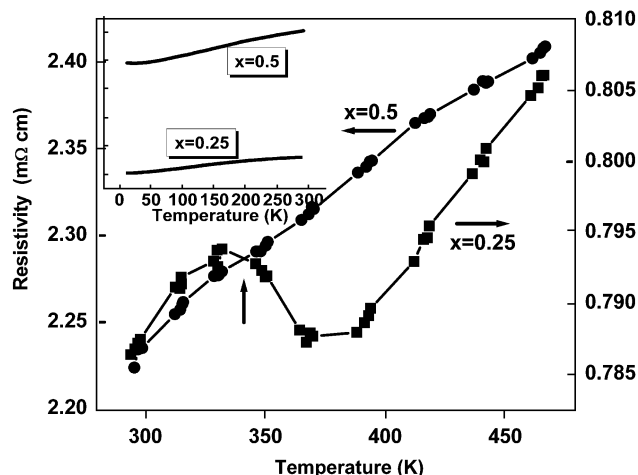


Fig. 4. Temperature dependence of the resistivity for $\text{Mn}_3\text{Ga}_{0.75}\text{Si}_{0.25}\text{N}$ (■) and $\text{Mn}_3\text{Ga}_{0.5}\text{Si}_{0.5}\text{N}$ (●).

- ⁴K. Kamishima, T. Goto, H. Nakagawa, N. Miura, M. Ohashi, N. Mori, T. Sasaki, and T. Kanomata, "Giant Magnetoresistance in the Intermetallic Compound Mn_3GaC ," *Phys. Rev. B*, **63**, 024426, 6pp (2000).
- ⁵E. O. Chi, W. S. Kim, and N. H. Hur, "Nearly Zero Temperature Coefficient of Resistivity in Antiperovskite Compound CuNMn_3 ," *Solid State Commun.*, **120**, 307–10 (2001).
- ⁶K. Asano, K. Koyama, and K. Takenaka, "Magnetostriiction in Mn_3CuN ," *Appl. Phys. Lett.*, **92**, 161909, 3pp (2008).
- ⁷E. F. Bertaut and D. Fruchart, "Neutron Diffraction of Mn_3GaN ," *Solid State Commun.*, **6** [5] 251–6 (1968).
- ⁸Y. Sun, C. Wang, and Y. C. Wen, "Negative Thermal Expansion in $\text{Mn}_3\text{Ga}(\text{Ge,Si})\text{N}$ Anti-perovskite Materials," *Mater. Sci. Forum*, **561–565**, 557–62 (2007).
- ⁹Y. Sun, C. Wang, Y. C. Wen, K. G. Zhu, and J. T. Zhao, "Lattice Contraction and Magnetic and Electronic Transport Properties of $\text{Mn}_3\text{Zn}_{1-x}\text{Ge}_x\text{N}$," *Appl. Phys. Lett.*, **91**, 231913, 3pp (2007).
- ¹⁰R. J. Huang, L. F. Li, F. S. Cai, X. D. Xu, and L. H. Qian, "Low-Temperature Negative Thermal Expansion of the Antiperovskite Manganese Nitride Mn_3CuN Codoped with Ge and Si," *Appl. Phys. Lett.*, **93**, 081902, 3pp (2008).
- ¹¹C. Dong, "PowderX: Windows-95-based Program for Powder X-ray Diffraction Data Processing," *J. Appl. Cryst.*, **32**, 838–39 (1999).
- ¹²K. Takenaka and H. Takagi, "Magnetovolume Effect and Negative Thermal Expansion in $\text{Mn}_3(\text{Cu}_{1-x}\text{Ge}_x)\text{N}$," *Mater. Trans.*, **47** [3] 471–74 (2006).
- ¹³J. P. Jardin and J. Labbe, "Phase Transitions and Band Structure in Metallic Perovskites (Carbides and Nitrides)," *J. Solid State Chem.*, **46**, 275–93 (1983).
- ¹⁴Y. B. Li, W. F. Li, W. J. Feng, Y. Q. Zhang, and Z. D. Zhang, "Magnetic, Transport and Magnetotransport Properties of $\text{Mn}_{3+x}\text{Sn}_{1-x}\text{C}$ and $\text{Mn}_3\text{Zn}_y\text{Sn}_{1-y}\text{C}$ Compounds," *Phys. Rev. B*, **72**, 024411, 8pp (2005).
- ¹⁵D. Fruchart and E. F. Bertaut, "Magnetic Studies of the Metallic Perovskite-Type Compounds of Manganese," *J. Phys. Soc. Jpn*, **44** [3] 781–91 (1978).
- ¹⁶S. Iikubo, K. Kodama, K. Takenaka, H. Takagi, and S. Shamoto, "Magnetovolume Effect in $\text{Mn}_3\text{Cu}_{1-x}\text{Ge}_x\text{N}$ related to the Magnetic Structure: Neutron Powder Diffraction Measurements," *Phys. Rev. B*, **77**, 020409(R), 4pp (2008).
- ¹⁷S. Iikubo, K. Kodama, K. Takenaka, H. Takagi, M. Takigawa, and S. Shamoto, "Local Lattice Distortion in the Giant Negative Thermal Expansion Material $\text{Mn}_3\text{Cu}_{1-x}\text{Ge}_x\text{N}$," *Phys. Rev. Lett.*, **101**, 205901, 4pp (2008). □